# Optimization of FRET algorithms for sensitized-emission FRET detection

**Sheng Wang (王 盛), Qiong Wu (吴 琼), and Zichun Hua (华子春)***

*State Key Laboratory of Pharmaceutical Biotechnology, Department of Biochemistry, College of Life Sciences and School of Stomatology, Affiliated Stomatological Hospital, Nanjing University, Nanjing 210093, China*

**Corresponding author: zchua@nju.edu.cn*

Received October 26, 2011; accepted February 12, 2012; posted online April 12, 2012

Sensitized-emission fluorescence resonance energy transfer (FRET) detection method based on three-channel fluorescence microscopy is widely used. Several FRET algorithms, such as $N_{FRET}$, $FRET_N$, FR, $FRET_R$, and $F^C$/Df, are developed recently to quantitatively gauge and compare FRET signals between different experimental groups. However, the algorithms are difficult to choose and interpret. In this letter, we optimize the suitable yellow fluorescent protein (YFP) to cyan fluorescent protein (CFP) concentration ratio range for the above FRET algorithms. We also test the effect of YFP-to-CFP concentration ratio on the calculated energy transfer efficiency $E$ and use the optimized FRET algorithms in the analysis of fas-associated protein with death domain (FADD) self-association directly in living cells.

*OCIS codes:* 170.2655, 170.2520, 170.1530.

*doi: 10.3788/COL201210.071701.*

Fluorescence resonance energy transfer (FRET) is a technique used to measure the interaction between two molecules labeled with two different fluorophores by the transfer of energy from the excited donor to the acceptor. FRET involves the transfer of energy from a fluorescence donor in its excited state to another excitable acceptor. In biological application, this technique can be used to gauge protein–protein interaction in living cells[1]. Cyan fluorescence protein (CFP) and yellow fluorescence protein (YFP) are a commonly used fluorescence donor and acceptor pair for tagging interested protein for live cell FRET imaging[2]. When FRET occurs, emission of the donor is decreased, whereas that of the acceptor is increased (sensitized emission). Many methods have been applied recently in measuring FRET *in vivo*, such as sensitized emission measurement[3], acceptor photobleaching measurement[4], spectral FRET measurement[5], and fluorescence lifetime imaging microscopy (FLIM)-FRET measurement[6]. Sensitized emission FRET measurement based on three-channel fluorescence microscopy, with its easy conduction and high spatiotemporal resolution for live cell FRET imaging, is commonly and widely used. Spectral cross-talk and spectral bleed-through, and variable CFP-to-YFP expression ratio may complicate the detection of FRET signals[7]. Therefore, many algorithms have been developed recently for the correction and determination of the FRET signals, such as $N_{FRET}$, $FRET_N$, FR, $FRET_R$, and $F^C$/Df[8−12]. In this letter, we characterize and optimize the YFP-to-CFP concentration ratio for each of the algorithms mentioned above, and then test the effect of YFP-to-CFP concentration ratio on the calculated energy transfer efficiency $E$. Finally, we analyze the fas-associated death domain protein (FADD) self-association in living cells using the optimized FRET algorithms.

The expression vectors for CFP- or YFP-tagged FADDs were constructed by inserting full length FADD in-frame with CFP-C1 and YFP-C1 (Clontech) vectors. The coding of vectors pECFP-YFP for the CFP-YFP fusion protein was generated by inserting YFP cDNA into CFP-C1 vectors. All the constructs were sequenced to ensure correct reading frame, orientation, and sequences. Spectroscopic measurements using a fluorescence spectrophotometer (F-7 000, Hitachi) revealed no spectral change for the CFP and YFP fluorescence in the tagged protein.

Hela cell line was grown in Dulbecco's modified Eagle's medium containing 10% fetal bovine serum and antibiotics in a 5% $CO_2$ incubator. Exponentially growing cells were dispersed with trypsin, seeded at $2\times10^5$ cells per 35 mm glass bottom dish in 1.5 ml of culture medium. The transfection of CFP and YFP fusion protein constructs was carried out using the calcium phosphate precipitation method.

Hela cells were plated onto 0.17-mm-thick bottom glass dishes and were transient transfected using the calcium phosphate precipitation method 24 h later. The cell were washed twice with PBS (PH 7.4), then covered with 1 ml fresh medium. Images were taken with an inverted microscope (IX81, Olympus) equipped with a 60×NA=1.45 oil immersion objective lenses and cooled charge-coupled devices. Excitation light was delivered by an X-cite light source. For imaging, Image-pro Plus software version 6.0 (Media Cybernetics) was used. In most experiments, the excitation intensity was attenuated down to 25% of the maximum power of the light source. Images were acquired using 1×1 binning mode and 400 integration time. For quantitative FRET measurements, the methods of sensitized FRET have been in detail described in Refs. [13–15]. Images were acquired sequentially through YFP, FRET, and CFP filter channels. Here, the filter sets used were YFP (S500/20 nm; Q5 15lp; S 535/30 nm, Chroma); CFP (S436/20 nm; Q4 55lp; S480/40 nm, Chroma); FRET(S436/20 nm; Q4 55lp; S535/30 nm, Chroma). The background images were removed from the raw images before carrying out FRET calculation.

Many algorithms have been developed recently based on three-channel FRET microscopy to gauge FRET signals[16]. In this letter, we used the two-letter sym-

 

bols defined by Gordon *et al.*[9] to depict the signals from different optical channels of fluorescence microscopy. In brief, the first uppercase letter representing the filter set is D for the donor filter set, F for the FRET filter set, and A for the acceptor set. The second lowercase letter indicates the fluorochromes present in the specimen: d for donor only, a for acceptor only, and f for both donor and acceptor being present (which makes FRET possible). For example, Dd represents the donor signal detected by the donor filter set, Ad represents the donor signal detected by the acceptor filter set, and Ff represents the signal detected by FRET filter set when donor and acceptor are present in the sample. In our system, the signal cannot be detected using YFP filter set when only CFP- or CFP-tagged proteins are present in the sample. In addition, the signal cannot be detected using CFP filter when only YFP- or YFP-tagged proteins are present in the sample. Therefore, we used the two-letter symbols to express the simplified FRET algorithms widely used as[17]

$$\begin{aligned} \mathrm{F^C} &= \mathrm{Ff} - \mathrm{Df}^*(\mathrm{Fd/Dd}) - \mathrm{Af} * (\mathrm{Fa/Aa}) \\ &= \mathrm{Ff} - \mathrm{b} * \mathrm{Df} - \mathrm{a} * \mathrm{Af}, \quad (1) \\ \mathrm{N_{FRET}} &= \mathrm{F^C}/(\mathrm{Df} * \mathrm{Af})^{1/2}, \quad (2) \\ \mathrm{FRET_N} &= \mathrm{F^C}/(\mathrm{Df} * \mathrm{Af}), \quad (3) \\ \mathrm{FR} &= (\mathrm{Ff} - \mathrm{b} * \mathrm{Df})/\mathrm{a} * \mathrm{Af}, \quad (4) \\ \mathrm{FRET_R} &= \mathrm{Ff}/(\mathrm{b} * \mathrm{Df} - \mathrm{a} * \mathrm{Af}), \quad (5) \\ &\mathrm{F^C/Df}, \quad (6) \end{aligned}$$

where b = Fd/Dd is the spectral bleed-through parameter between the CFP and FRET channels and a = Fa/Aa is the spectral cross-talk parameter between the YFP and FRET channels, respectively. In our system, a=0.16±0.02, b=0.22±0.01, and $\mathrm{F^C}$ represents the corrected FRET signal.

We also calculated the energy transfer efficiency $E$. The energy transfer efficiency was calculated as the ratio of the donor image in the presence ($I_{\mathrm{DA}}$) and absence ($I_{\mathrm{D}}$) of acceptor[18]

$$E = 1 - I_{\mathrm{DA}}/I_{\mathrm{D}} = 1 - \mathrm{Df}/(\mathrm{Df} + \mathrm{F^C} * G^{-1}), \quad (7)$$

$$G = (Q_{\mathrm{a}}/Q_{\mathrm{d}}) * (\psi_{\mathrm{aa}}/\psi_{\mathrm{dd}}), \quad (8)$$

where $G$[9] is the factor relating the loss of donor emission due to FRET in the donor filter set to the gain of acceptor emission due to FRET in the FRET filter set, $Q_{\mathrm{a}}$ and $Q_{\mathrm{d}}$ are the quantum yields of the acceptor and donor, respectively, and $\psi_{\mathrm{aa}}$ and $\psi_{\mathrm{dd}}$ are the collection efficiencies in the acceptor and donor channels, respectively. The quantum yield of ECFP is 0.37 and that of the EYFP is 0.6[19]. The normalized spectral sensitivity of the donor channel is 12 and that of the acceptor channel is 8. Therefore, in our system, $G$=1.0, and $E$ can be calculated as

$$E = 1 - \mathrm{Df}/(\mathrm{Df} + \mathrm{F^C}).$$

All results are expressed as means ± S.E values. The significance of differences among the means of various groups was determined by Student's $t$ test.

We used Hela cell co-expressing CFP and YFP proteins as negative control and cell co-expressing CFP-YFP fusion protein as positive control to test whether our three-channel microscopy system can reliably detect and quantify FRET signals *in vivo*. In addition, $\mathrm{N_{FRET}}$, $\mathrm{FRET_N}$, FR, $\mathrm{FRET_R}$, and $\mathrm{F^C/Df}$ algorithms were used to quantitatively gauge and compare FRET signals between the positive and negative control groups. As shown in Table 1, cells co-expressing CFP and YFP gave very low $\mathrm{N_{FRET}}$, $\mathrm{FRET_N}$, FR, $\mathrm{FRET_R}$, and $\mathrm{F^C/Df}$ values, whereas cell co-expressing CFP-YFP fusion protein gave significantly high $\mathrm{N_{FRET}}$, $\mathrm{FRET_N}$, FR, $\mathrm{FRET_R}$, and $\mathrm{F^C/Df}$ values ($P$<0.01). ECFP and EYFP are monomerized fluorescent protein; thus, randomly expressed CFP and YFP protein in cells will not have FRET. Thus, we theorized that overexpression of CFP and YFP together cannot result in FRET between CFP and YFP. In addition, we found that Hela cells expressing CFP-YFP indicated significant increase in $\mathrm{N_{FRET}}$, $\mathrm{FRET_N}$, FR, $\mathrm{FRET_R}$, and $\mathrm{F^C/Df}$ values. CFP-YFP fusion protein has the CFP and YFP ratio of 1:1 and a short flexible linker peptide between the CFP and YFP protein. CFP-YFP had the strongest FRET detected by our system. Based on the above mentioned FRET algorithms, values calculated from each algorithm showed significant difference between positive control and negative control experimental groups. In the $\mathrm{F^C}$ image in Fig. 1, significant FRET signal is evident in both cytoplasm and nuclear of cells expressing CFP-YFP fusion protein, whereas cells co-expressing CFP and YFP show no FRET signal. Hela cells expressing the indicated fusing proteins are imaged with FRET microscopy through CFP, YFP, and FRET channels. $\mathrm{FRET^c}$ is calculated as described in the Materials and Methods section and presented as pseudo-color images. All colors are arbitrarily assigned to indicate

**Table 1. Calculation of FRET for Positive and Negative Controls**

| Algorithm | $\mathrm{N_{FRET}}$ | $\mathrm{FRET_N}$ | $\mathrm{F^C/Df}$ | FR | $\mathrm{FRET_R}$ | $E$ | $n$ |
|---|---|---|---|---|---|---|---|
| CFP-YFP | | | | | | | 90 |
| Mean | 0.72 | 0.00149 | 0.77 | 5.18 | 2.88 | 43% | |
| S.E | 0.006 | 0.00012 | 0.01 | 0.02 | 0.02 | 0.40% | |
| CFP+YFP | | | | | | | 82 |
| Mean | 0.0036 | 0.0000071 | 0.0025 | 1.03 | 1.0079 | 0.24% | |
| S.E | 0.0017 | 0.0000045 | 0.0011 | 0.01 | 0.0034 | 0.10% | |
| $t$ test | $P < 0.01$ | $P < 0.01$ | $P < 0.01$ | $P < 0.01$ | $P < 0.01$ | $P < 0.01$ | |

$P < 0.01$ versus co-expression of CFP and YFP in Hela cells.

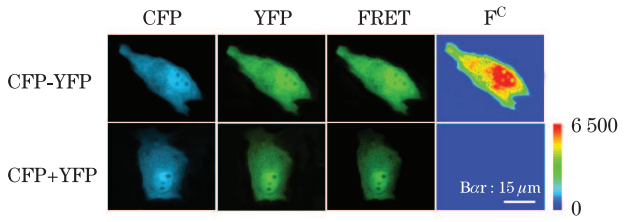


Fig. 1. (Color online) Visualization of protein interaction under fixed YFP-to-CFP stoichiometry.

signal strength. Hela cells transfected with CFP-YFP serve as the positive control, whereas cells co-transfected with CFP and YFP as the negative control. Therefore, in our system, these algorithms can all be used to indicate the occurrence of FRET signals reliably detected in our three-channel microscopy system.

The CFP-YFP fusion protein has a fixed CFP and YFP expression level, so FRET signal can be easily detected and quantified. However, in a real FRET experiment, although we can adjust the amount of plasmid of CFP and YFP tagged protein for transfection, we cannot control the expression level of CFP and YFP tagged protein in individual cell. Therefore, the YFP to CFP concentration ratio can differ from one cell to another. We co-expressed CFP-YFP and CFP or CFP-YFP and YFP to intentionally change the YFP to CFP concentration ratio in Hela cells to determine whether varying YFP-to-CFP concentration ratio can influence the results getting from algorithms mentioned above. Because we expressed CFP-YFP fusion protein, FRET signal should be detected by our system. As shown in Fig. 2, when the YFP-to-CFP concentration ratio is less than 1, the FR values remain approximately constant and at the same level with the FR values obtained from the fixed YFP-to-CFP stoichiometry group. As the YFP-to-CFP concentration ratio increases above 1, the FR values drop dramatically. As the YFP-to-CFP concentration ratio increases above 13, the FR values are approximate at the same level as the negative control (data not shown). This data trend is contrary to that of the $F^C$/Df algorithm. When YFP-to-CFP concentration ratio is above 1, the values from the $F^C$/Df algorithm remain approximately constant, and when YFP-to-CFP concentration ratio is below 1, the values from $F^C$/Df algorithm drop dramatically. Another algorithm of $FRET_R$ values remains approximately constant at the same level as the $FRET_R$ values obtained from fixed YFP-to-CFP stoichiometry group when the YFP-to-CFP concentration ratio is approximately 1. As the YFP-to-CFP concentration ratio increases above 1 or decreases below 1, $FRET_R$ values drop dramatically. This data trend is the same as that of $N_{FRET}$ algorithm. When we used the $FRET_N$ algorithm to gauge FRET, we found that $FRET_N$ values had great variability and no specific data trend as the YFP-to-CFP concentration ratio decreases or increases. We also tested the calculated FRET $E$ under various YFP-to-CFP concentration ratios. As shown in Fig. 2, $E$ remains constant as the YFP-to-CFP concentration ratio is above 1.

FADD is an adaptor molecule for the death receptor subfamily mediating death receptor signal from plasma membrane to cytoplasm[20]. FADD protein has the potential to be highly oligomeric and its *in vitro* self-association has been reported previously[21]. We analyzed the FADD self-association directly in living cells using the above optimized FRET algorithms. We chose the cells in the optimized YFP-to-CFP concentration ratio range for FRET measurement and statistical analysis.

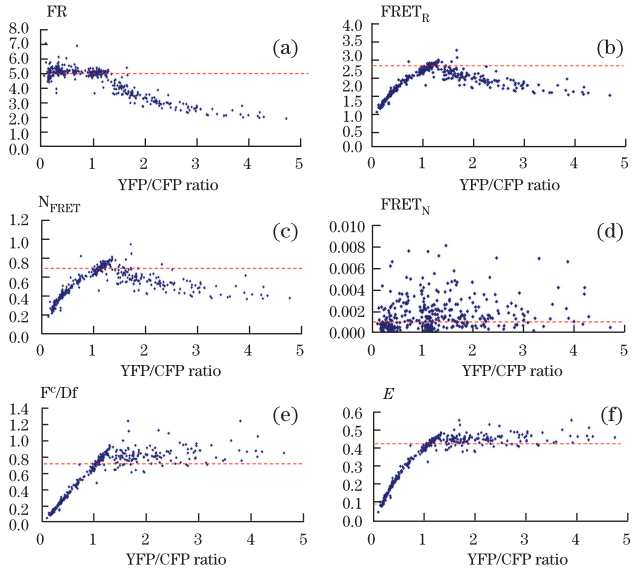


Fig. 2. (Color online) Influence of YFP-to-CFP concentration ratio on the energy transfer efficiency $E$ and values calculated by various FRET algorithms. The red dotted line indicates the mean data of cells expressing CFP-YFP fusion protein calculated from each algorithm.

**Table 2. Calculation of FRET for FADD Self-association Analysis**

| Algorithms | $N_{FRET}$ | $FRET_N$ | $F^C$/Df | FR | $FRET_R$ | $E$ | $n$ |
|---|---|---|---|---|---|---|---|
| CFP-FADD+YFP-FADD | | | | | | | 30 |
| Mean | 0.093 | 0.00030 | 0.083 | 1.64 | 1.23 | 7% | |
| S.E | 0.017 | 0.00005 | 0.016 | 0.01 | 0.04 | 1% | |
| CFP-FADD+YFP | | | | | | | 40 |
| Mean | 0.0043 | 0.0000084 | 0.0038 | 1.05 | 1.0098 | 0.31% | |
| SE | 0.0031 | 0.0000062 | 0.0016 | 0.01 | 0.0042 | 0.12% | |
| CFP+YFP-FADD | | | | | | | 40 |
| Mean | 0.0039 | 0.0000075 | 0.0036 | 1.04 | 1.0084 | 0.29% | |
| S.E | 0.0014 | 0.0000053 | 0.0013 | 0.01 | 0.0032 | 0.11% | |
| $t$ test | $P < 0.01$ | $P < 0.01$ | $P < 0.01$ | $P < 0.01$ | $P < 0.01$ | $P < 0.01$ | |

$P$ <0.01 versus co-expression of CFP-FADD and YFP or YFP-FADD and CFP in Hela cells.

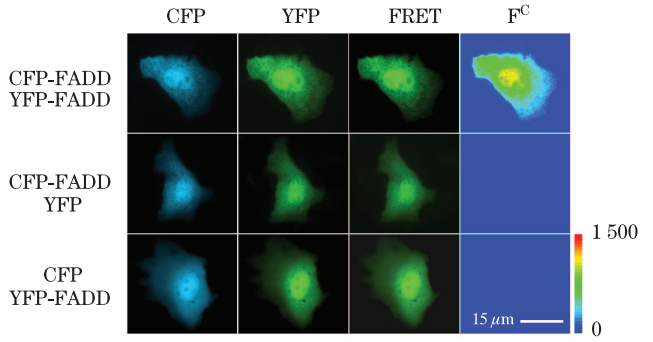


Fig. 3. FRET imaging to visualize the self-association of FADD in living cells.

As shown in Table 2, cells co-expressing CFP-FADD and YFP-FADD show significantly high $N_{FRET}$, $FRET_N$, FR, $FRET_R$, and $F^C$/Df values compared with cells co-expressing CFP- and YFP-tagged FADD or YFP- and CFP-tagged FADD as negative control. This randomly distributed self-interaction signals in the whole cell body can be visualized by $F^C$ pseudo-color image as shown in Fig. 3. These data clearly demonstrate that FADD can have specific self-association in living cells.

In conclusion, we optimize the YFP-to-CFP concentration ratio range for the algorithms discussed above. Optimization of YFP-to-CFP concentration ratio range when choosing suitable FRET algorithms are more suitable for precise FRET signal detection based on three-channel fluorescence microscopy.

This work was supported by the National "973" Program of China (Nos. 2011CB933502 and 2012CB967004,), the National Natural Science Foundation of China (Nos. 81121062, 50973046, 31071196, 81072712, and 31070706), and the Jiangsu Provincial Natural Science Foundation (Nos. BK2010046, BZ2010074, BK2011228, BK2011573, and BZ2011048).

## References

1. M. C. Dinger, J. E. Bader, A. D. Kobor, A. K. Kretzschmar, and A. G. Beck-Sickinger, J. Biol. Chem. **278,** 10562 (2003).
2. K. Truong and M. Ikura, Curr. Opin. Struc. Biol. **11,** 573 (2001).
3. S. Qiu, Y. Hua, F. Yang, Y. Chen, and J. Luo, J. Biol. Chem. **280,** 24923 (2005).
4. L. Song, E. J. Hennink, I. T. Young, and H. J. Tanke, Biophys. Jouranl **68,** 2588 (1995).
5. C. L. Takanishi, E. A. Bykova, W. Cheng, and J. Zheng, Brain Res. **1091,** 132 (2006).
6. Y. Chen, J. D. Mills, and A. Periasamy, Differentiation **71,** 528 (2003).
7. C. Barney and G. Danuser, Biophys. Jouranl **84,** 3992 (2003).
8. Z. Xia and Y. Liu, Biophys. Journal **81,** 2395 (2001).
9. G. W. Gordon, G. Berry, X. H. Liang, B. Levine, and B. Herman, Biophys. Journal **74,** 2702 (1998).
10. M. G. Erickson, B. A. Alseikhan, B. Z. Peterson, and D. T. Yue, Neuron **31,** 973 (2001).
11. E. G. D. Muller, B. E. Snydsman, I. Novik, D. W. Hailey, D. R. Gestaut, C. A. Niemann, E. T. O'Toole, T. H. Giddings, Jr., B. A. Sundin, and T. N. Davis, Mol. Biol. Cell **16,** 3341 (2005).
12. Z. Xia, Q. Zhou, J. Lin, and Y. Liu, J. Biol. Chem. **276,** 1766 ( 2001).
13. F. Zhang, G. Fu, C. Wang, L. Cao, H. Yang, G. Wang, Y. Chen, and C. He, Mol. Imaging Biol. **11,** 188 (2009).
14. D. C. Youvan, C. M. Silva, E. J. Bylina, W. J. Coleman, M. R. Dilworth, and M. M. Yang, Biotechnology **3,** 1 (1997).
15. T. Sorkina, S. Doolen, E. Galperin, N. R. Zahniser, and A. Sorkin, J. Biol. Chem. **278,** 28274 (2003).
16. R. N. Day, A. Periasamy, and F. Schaufele, Methods. **25,** 4 (2001).
17. G. Fu, H. Yang, C. Wang, F. Zhang, Z.You, G. Wang, C. He, Y. Chen, and Z. Xu, Biochem. Biophys. Res. Commun. **346,** 986 (2006).
18. M. Elangovan, W. Horst, Y. Chen, R. N. Day, M. Barroso, and A. Periasamy, Methods **29,** 58 (2003).
19. M. A. Rizzo, G. H. Springer, B. Granada, and D. W. Piston, Nat. Biotechnol. **22,** 445 (2004).
20. B. C. Barnhart, J. C. Lee, E. C. Alappat, and M. E. Peter, Oncogene **22,** 8634 (2003).
21. R. M. Siegel, D. A. Martin, L. Zheng, S. Y. Ng, J. Bertin, J. Cohen, and M. J. Lenardo, J. Cell. Biol. **141,** 1243 (1998).